Amino Acids (2009) 37:249–255
DOI 10.1007/s00726-008-0140-8

ORIGINAL ARTICLE

Cellular uptake of cationic gadolinium-DOTA peptide conjugates with and without N-terminal myristoylation

A. Sturzu · U. Klose · H. Echner · A. Beck · A. Gharabaghi · H. Kalbacher · S. Heckl

Received: 6 June 2008 / Accepted: 19 June 2008 / Published online: 17 July 2008

Abstract Cellular and nuclear uptake of dual labelled conjugates could be of great value for chemotherapy and cancer diagnostics. Therefore we designed conjugates in which gadolinium (Gd)-1,4,7,10-tetraazacyclododecane-1,4,7,10-tetraacetic acid (DOTA), a contrast agent for magnetic resonance imaging and fluorescein isothiocyanate (FITC), a fluorescence marker were coupled to membrane translocation sequences (MTS). The MTSs we employed were the third helix of the Antennapedia homeodomain, the HIV-1 Tat peptide and the N-myristoylated HIV-1 Tat peptide. We used confocal laser scanning microscopy, fluorescence activated cell sorting, magnetic resonance imaging (MRI) and viability tests to examine the cellular and nuclear uptake of these conjugates into U373 glioma cells, as well as their cytotoxic effects. We found that the Antennapedia conjugate was taken up by no more than 20% of the cells. The HIV-1 Tat conjugate showed even lower uptake into less than 3% of cells. Interestingly, N-myristoylation of the HIV-1 Tat conjugate drastically improved its cellular uptake. Up to 70% of cells showed cellular and nuclear uptake of the N-myristoylated HIV-1 Tat conjugate. Conjugate cytotoxicity appears to correlate with cellular uptake.

Keywords N-myristoylation · HIV-1 Tat · Penetratin · Tetraazacyclododecane-tetraacetic acid · Gadolinium · Cellular uptake · Chemotherapy

A. Sturzu (✉) · H. Echner · H. Kalbacher
Peptide Synthesis Laboratory,
Interfaculty Institute of Biochemistry, University of Tübingen,
Hoppe-Seyler-Str.4, 72076 Tübingen, Germany
e-mail: alexsturzu@yahoo.de

A. Sturzu · U. Klose · S. Heckl
Department of Neuroradiology,
University of Tübingen, Tübingen, Germany

A. Beck
Center for Clinical Mass Spectrometry,
Heilbronn, Germany

A. Gharabaghi
Department of Neurosurgery,
University of Tübingen, Tübingen, Germany

Introduction

Intracellular accumulation of conjugates carrying two detection markers for different imaging techniques (fluorescein isothiocyanate (FITC) and gadolinium (Gd) 1,4,7,10-tetraazacyclododecane-1,4,7,10-tetraacetic acid (DOTA)) are of great interest for intracellular diagnostics. FITC is a commonly used fluorescence dye. Gd-DOTA is an extracellular contrast agent for magnetic resonance imaging (Le Mignon et al. 1990).

An FITC-labelled Gd-DOTA complex could not traverse the cell membrane (Sturzu et al. 2008).

Due to the fact, that two cargoes have to be translocated across the cellular membrane, it is of the utmost importance to design a potent transport unit for magnetic resonance imaging.

Such a unit can also be of great value for the combined therapeutic and diagnostic use (e.g. coupling of chemotherapeutic agents or antibodies to the bimodal contrast agent).

In the present work, three membrane translocation sequences (Penetratin, HIV-1 Tat, N-myristoylated HIV-1 Tat) were coupled to a small tetrapeptide conjugate carrying FITC and Gd-DOTA.

In the dual labelled conjugate C1 we used Penetratin, the third helix of the Antennapedia homeodomain (a *Drosophila*

transcription factor). Penetratin is internalized into cells by a receptor-independent mechanism (Derossi et al. 1996).

The membrane translocation sequence in conjugate C2 was the HIV-1 Tat peptide. Either Gd-DOTA or FITC has been successfully internalized into mammalian cells when coupled to the HIV-1 Tat peptide (Bhorade et al. 2000; Prantner et al. 2003). However, these previous studies employed monolabelled conjugates.

By modification of our dual labelled HIV-1 Tat conjugate C2 through N-myristoylation, we obtained conjugate C3.

Myristic acid is a saturated linear fatty acid (tetradecanoic acid, $C_{14}H_{28}O_2$, MW: 228.4).

N-terminal myristoylation is a naturally occurring protein modification and has been found to be essential for membrane localization of proteins (Vaandrager et al. 1996). Also, the N-terminal myristic acid can act as membrane anchor (Desmeules et al. 2002; Sankaram 1994).

These properties indicate that myristoylation may enhance cellular uptake of peptide conjugates. It has been shown that even an anionic heptaglutamic acid chain was incorporated into human carcinoma cells when myristoylated on a lysine side chain at the C-Terminus (Nelson et al. 2007).

It is assumed, that the numerous cationic amino acids in the Antennapedia conjugate interact with the negatively charged phospholipids of the cell membrane leading to cellular uptake (Christiaens et al. 2004).

So adding further cationic amino acids like polyarginine to the above mentioned membrane translocation sequences may also enhance cellular uptake.

However, previous investigations showed that a Gd-DOTA-FITC-conjugate in which four arginines were added to the SV40 T antigen nuclear localization peptide still left over 60% of human glioma cells unstained (Sturzu et al. 2008).

Compared to the strategy of adding cationic amino acids to the conjugates, N-myristoylation has two major advantages.

Synthesis of conjugates is quicker and cheaper and N-myristoylation harbors less allergenic potential than a conjugate carrying a long polyarginine chain (Minnicozzi et al. 1995).

Following conjugates were used:

C1. Penetratin coupled to FITC and Gd-DOTA: RQIKIWFQNRRMKWKK-K(FITC)GGK(Gd-DOTA).

C2. The basic domain $Tat_{49–57}$ of HIV-1 (Vivès et al. 1997; Wender et al. 2000) with FITC and Gd-DOTA: RKKRRQRRR-K(FITC)GGK(Gd-DOTA).

C3. Conjugate C2 carrying myristic acid (X) as N-terminal modification: X-RKKRRQRRR-K(FITC)GGK(Gd-DOTA).

Cellular uptake of these conjugates into human U373 glioma cells was examined using confocal laser scanning microscopy (CLSM), fluorescence activated cell sorting (FACS) and magnetic resonance imaging (MRI).

It was examined whether N-myristoylation may enhance cellular uptake of Gd-DOTA-FITC conjugates.

Materials and methods

Synthesis of DOTA conjugates

Synthesis was performed by solid phase peptide synthesis on an Eppendorf ECOSYN P peptide synthesizer (Eppendorf-Biotronik, Hamburg, Germany) employing the fmoc strategy. The amino group was protected with fmoc (9-fluorenylmethyloxycarbonyl) which can be cleaved off under alkaline conditions. Tentagel S rink amid resin (Rapp-Polymere, Tübingen, Germany) was used as carrier material. Synthesis was carried out on a scale of 0.1 mmol/l. Four time excess of fmoc-protected amino acids were coupled to the resin in a 40-min reaction using 4 equivalents of TBTU (2-(1H-benzotriazole-1-yl)-1,1,3,4-tetramethyluronium tetrafluoroborate) as coupling reagent and 8 equivalents of DIPEA (diisopropylethylamine) as an adjuvant base. Amino acid side chains were protected by following protective groups: Lysine: tert.-butyl-oxycarbonyle (tBoc), Arginine: Pbf (N^6-2,2,4,6,7-pentamethyl-dihydrobenzofurane-5-sulfonyl).

Lysine side chains designated for DOTA were protected with Mmt (4-methoxytrityl). Lysine side chains carrying a fluorescein urea derivate were protected with Dde (1-(4,4-dimethyl-2,6-dioxocyclohex-1-ylidene)-ethyl). After each coupling, the fmoc protective group was cleaved off by a 25% piperidine solution in DMF (dimethyl-formamide) in an 11-min reaction step.

Peptides were sequentially synthesized, beginning at the C-terminus.

For the N-myristoylated conjugate C3, myristic acid (Sigma-Aldrich, Taufkirchen, Germany) was coupled to the amino acid chain in the final step of peptide elongation. The conditions for this coupling reaction were identical to those used for amino acid coupling.

For introduction of DOTA (1,4,7,10-tetraazacyclododecane), the Mmt protective group was cleaved off by repeated treatment with a solution of 1% TFA (trifluoro acetic acid) and 1% TIPS (triisopropylsilane) in DCM during 1 h. After several washing steps with DMF and neutralising of the resulting TFA-salt with DIPEA the

deprotected side chain was accessible for DOTA coupling. Coupling was carried out with 3 equivalents of 1,4,7,10-tetraacacyclododecane-1,4,7-tris(tert.butylester)-10-acetic acid (Macrocyclics, Dallas, USA), 3 equivalents of TBTU and 6 equivalents of DIPEA during 1.5 h at room temperature. Then the Dde side chain protective group was cleaved off by repeatedly treating the resin with a solution of 2.5% hydrazinhydrate in DMF over the course of 1 h. After several washing steps with DMF, the fluorescein urea derivate was coupled to the peptide using 0.5 mM fluoresceine-5-isothiocyanate with an equal amount of DIPEA in DMSO (dimethylsulfoxide) at room temperature over night. The peptide resin was then washed with DMF, methanol and DCM.

Cleavage of the remaining side chain protective groups was carried out simultaneously with cleavage of the peptide from the resin in one final step. The dry resin was therefore stirred at room temperature for 3 h in a mixture of 12 ml TFA, 0.3 ml ethandithiol (EDT), 0.3 ml anisole, 0.3 ml water and 0.1 ml TIPS.

The peptide was then precipitated with cold pure diethyl ether, filtered, washed again with ether and dried in vacuum. The resulting raw peptide was purified via semipreparative HPLC (high performance liquid chromatography).

Equimolar amounts of Gd-chloride solution were applied to the DOTA-peptides, pH was set to 5.2–5.6 using 0.1 M NaOH and the mixture was stirred at 50°C for 5 h. After neutralisation with a few drops of acetic acid, the solution was lyophilised. The resulting Gd-containing and Gd-free DOTA-conjugates were shown to be ≥97% pure by analytical HPLC, and their molecular weights were determined by electrospray ionization mass spectrometry (ESI-MS).

Electrospray ionization mass spectrometry (ESI-MS)

The conjugates (Table 1) were analyzed by ESI-MS on an Esquire3000 + ion trap mass spectrometer (Bruker-Daltonics, Bremen, Germany). They were dissolved in 40% ACN, 0.1% formic acid in water (v/v/v) (20 pmol/µl) and constantly infused using a syringe pump (5 µl/min flow rate). Mass spectra were acquired in positive ion mode. Dry gas (6 l/min) temperature was set to 325°C, the nebulizer to 20.0 psi, and the electrospray voltage to −3,700 V.

Confocal laser scanning microscopy (CLSM)

Human U373 glioma cells were grown to 80% confluency in 75 cm^2 cell culture flasks (Corning Costar, Bodenheim, Germany) at 37°C in an atmosphere of 5% CO_2 (v/v).

Accutase™ (PAA laboratories) was added to detach the cells which were harvested and subsequently transferred to 16-well plates (NUNC, Wiesbaden, Germany) (37°C, 5% CO_2 (v/v)). Cells (80% confluency) were incubated with

Table 1 Conjugates C1–C3

C1	RQIKIWFQNRRMKWKKK(FITC)GGK(GdDOTA)
C2	RKKRRQRRRK(FITC)GGK(GdDOTA)
C3	XRKKRRQRRRK(FITC)GGK(GdDOTA)

Single-letter amino acid code: *R* arginine; *Q* glutamine; *I* isoleucine; *K* lysine; *W* tryptophan; *F* phenylalanine; *N* asparagine; *M* methionine; *X* myristic acid (tetradecanoic acid); *DOTA* 1,4,7,10-tetraazacyclododecane-1,4,7,10-tetraacetic acid; *Gd* gadolinium; *FITC* fluorescein isothiocyanate

Dulbecco′s phosphate buffered saline (D-PBS; GIBCO; Invitrogen, Germany) alone (negative control) and with 260 µM solutions of the conjugates in D-PBS for 20 min. After this, the cells were rinsed three times with buffer and then incubated with RPMI 1640 Ready Mix Medium (PAA laboratories) again.

PI was added to the medium (1–5 µmol l^{-1} PI; Molecular Probes, Eugene, OR, USA) to detect cells with damaged cell membranes.

The FITC-labelled conjugates were detected by confocal laser scanning microscopy.

Confocal laser scanning microscopy was performed on an inverted LSM 510 laser scanning microscope (Carl Zeiss) (objectives: LD Achroplan 40 × 0.6, Plan Neofluar 20 × 0.50, 40 × 0.75). For fluorescence excitation, the 488 nm line of an argon laser and the 543 nm line of a HeNe laser with appropriate beam splitters and barrier filters were used for FITC and PI, respectively. Superimposed images of FITC- and PI-stained samples were created by overlaying coincident views. All measurements were performed at least three times in living cells.

For live cell imaging, incubation was cut short to 10 min. After addition of PI to the medium, images of the same region were taken every minute for the first 10 min and at growing intervals for the next 50 min.

Evaluation of confocal laser scanning using the Image J software

Images of adherent cells were acquired (see confocal laser scanning) and converted to jpg format with the LSM Image Browser software (Carl Zeiss, Jena, Germany). Using the Image J software (Wayne Rasband, NIH, Bethesda, MD, USA) the mean brightness values of stained and non-stained cells (∼150 cells per incubation), as well as the mean brightness of the background were acquired and listed. The threshold for cell staining was observed at a brightness value equal to the background value +10%. Three independent incubations were evaluated and the results were listed.

PI staining was evaluated using pictures showing the fusion of the PI channel and the transmission channel. All PI-stained and non-stained cells in a picture sector (∼300

cells) were counted and the staining ratio was determined. This was performed for pictures of 3 independent incubations. Mean staining ratio and deviation are presented (Fig. 2a).

Magnetic resonance (MR) relaxometry

For MR relaxometry, human U373 glioma cells were grown in 75 cm^2 cell culture flasks (Corning Costar, Bodenheim Germany) (70% confluency). Accutase™ (PAA laboratories, Pasching, Austria) was added to achieve detachment of the cells, which were harvested and subsequently aliquoted into Eppendorf tubes (6×10^6 cells per tube). The cells in the first tube served as a control (PBS only). The cells in the other tubes were incubated with conjugates C1–C3 (260 µM). After a 20-min incubation period at 37°C in an atmosphere of 5% CO_2, the cells were washed three times in PBS and centrifuged at 800 rpm for 5 min.

In vitro imaging was performed with a 3 Tesla whole body MRI-system (Trio Magnetom, circular polarised knee coil, Siemens, Erlangen, Germany).

Sagittal T1-weighted MR images were obtained using the following spin echo sequence TR (repetition time): 200 ms, TE (echo time): 7.4 ms, flip angle 90°, averages: 1, concatenations: 2, measurements: 1, number of slices: 19, distance factor: 30%, slice thickness: 3 mm, field of view read: 180 mm, field of view phase: 100%, base resolution: 256, phase resolution: 100%, voxel size: 0.7 × 0.7 × 3.0 mm, scan time: 1:48 min.

T1 relaxation times were evaluated from signal intensities obtained by multiple axial spin echo measurements TR: 20–8,000 ms (50 different TR values), TE: 6.4 ms, flip angle 90°, averages: 1, measurements: 1, number of slices: 1, slice thickness: 1 mm, field of view read: 120 mm, field of view phase: 87.5, base resolution 128, phase resolution: 100%, voxel size: 0.9 × 0.9 × 1 mm.

Analyses and calculations were performed using a Matlab program (Math Works, Natick, MA, USA). T1 values were estimated by a two-parameter fit procedure.

All signal curves were examined and found to be monoexponential.

The investigations were performed in triplicate.

Flow cytometry

Fluorescence activated cell sorting (FACS) was performed using a Becton Dickinson FACSCalibur. 1×10^6 cells were incubated in 100 µl of conjugate solutions (260 µM in PBS) or PBS alone for 20 min. Then 300 µl FACS buffer (D-PBS containing 1% paraformaldehyde) was added. The samples were measured immediately. Approximately 25,000 events were recorded per sample. Fluorescence excitation was achieved by an Argon laser (488 nm). Fluorescence was detected using a 540–565 nm bandpass filter.

For FACS evaluation the mean FITC fluorescence intensity for each conjugate was acquired using the WinMDI software (Joseph Trotter, Scripps Research Institute, San Diego, CA, USA). All investigations were performed in triplicate and statistically evaluated.

Results

Synthesis of conjugates

We synthesized three FITC-labelled and gadolinium-containing DOTA (C1-C3) conjugates (Table 1). Their molecular masses were verified by electrospray ionisation mass spectrometry ((C1: calculated mass: 3,544.8 Da, measured mass: 3,545.5 Da); (C2: calculated mass: 2,638.4 Da, measured mass 2,637.6 Da); (C3: calculated mass 2,849.8 Da, measured mass 2,848.1 Da) (average masses)).

Fluorescence microscopy, flow cytometry and viability tests

Incubation with conjugate C1 produced weak staining with regard to the number of positive cells (16–18%, Figs. 1a, 2a) and staining intensity (Fig. 2b).

The application of conjugate C2 resulted in dramatically reduced staining (less than 3% of cells, Figs. 1a, 2a, b).

Conjugate C3 stained the majority of cells (60–69%, Figs. 1a, 2a, b).

A constant ratio of approximately 3 in 5 cells stained by conjugates C1 and C3 were nonviable, as shown by the nuclear uptake of propidium iodide (PI) (Figs. 1a, 2a).

Cell viability after incubation with conjugate C2 could not be evaluated due to the very low staining rate (FITC: 2–3%, PI: 0–1%).

Live cell imaging demonstrated, that after incubation with the N-myristoylated conjugate C3, cells with extensive membrane damage as a result of conjugate uptake (indicated by PI staining) show conjugate leakage into the extracellular space (Fig. 1b). Even several minutes after the incubation was stopped, stained intact cells started leaking conjugate C3 and taking up PI. Consecutively, only the nucleoli, the nuclear membrane and the cell membrane retained stronger staining. By contrast, stained intact cells (without PI) exhibited strong staining of the cytoplasm, cell nucleus, nucleoli and the nuclear membrane (Fig. 1c).

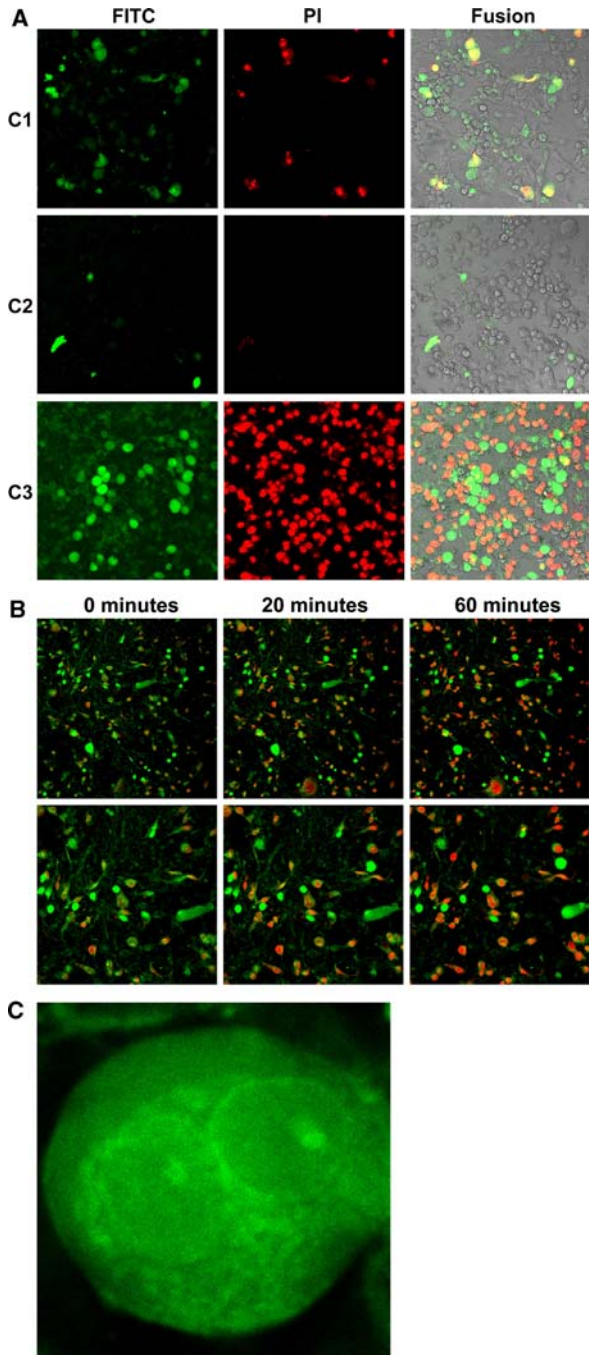

Fig. 1 CLSM images of human malignant U373 glioma cells. **a** Fluorescein isothiocyanate (FITC), propidium iodide (PI) and fusion images of cells incubated with conjugates C1–C3. While C1 leads to weak but definite FITC and PI staining, C2 shows only very few FITC stained cells and no noticeable PI staining. Incubation with conjugate C3 leads to strong FITC and PI staining. The PI stained cells exhibit much weaker cytoplasmic FITC staining than intact stained cells. **b** Live cell imaging. Overview images and magnifications of cells incubated with conjugate C3 at three different times. Immediately after the incubation only few cells show PI staining. After 20 and 60 min PI staining grows stronger while the FITC staining of the cells taking up PI grows weaker. **c** Close-up image after incubation with conjugate C3 shows the localization of the conjugate (cytoplasm, cell nucleus, nuclear membrane and nucleolus)

Flow cytometry confirmed the results of the confocal laser scanning microscopy. Incubation with conjugate C3 led to the highest mean fluorescence intensity, followed by conjugate C1. Intensity was lowest after incubation with conjugate C2 (Fig. 2b).

Magnetic resonance relaxometry

Monoexponential relaxation curves were fitted to the data points obtained from the axial T1 measurements (C1–C3).

T1 relaxation time values after incubation with all conjugates were considerably shortened compared to those obtained from the native control.

Shortening of T1 relaxation time was lowest after incubation with conjugate C2. Incubation with conjugate C1 resulted in stronger shortening of relaxation time. Incubation with conjugate C3 showed the greatest effect (Fig. 3a, b).

Discussion

We tried to achieve cytoplasmic and nuclear uptake of novel Gd-DOTA- and FITC-containing peptide conjugates.

Possible effects from the small tetrapeptide (KGGK, Table 1) carrying the FITC and Gd-DOTA markers could be excluded in a previous study (Sturzu et al. 2008).

Conjugate C1, in which the Gd-DOTA complex and FITC were bound to the third helix of the Antennapedia homeodomain, was transported into human U373 glioma cells. This was to be expected, as cellular uptake of Antennapedia conjugates into rat brain cells has already been described (biotin monolabel, Derossi et al. 1994). However, until now, Penetratin has not yet found use in studies with Gd-DOTA.

We could show for the first time that this dual labelled conjugate presents with a surprisingly low cellular uptake rate of only 16–18% (Figs. 2a, 3a).

It has also been shown that HIV-1 Tat peptide conjugates are internalized into human cells (Vivès et al. 1997; Bhorade et al. 2000; Prantner et al. 2003).

However, these conjugates were all monolabelled either with FITC or Gd-DOTA.

By contrast our dual labelled HIV-1 Tat peptide conjugate C2 showed only minimal uptake into no more than 3% of cells.

Both conjugates C1 and C2 showed lower cellular uptake than was to be expected considering the above mentioned previous research on monolabelled conjugates. Apparently, carrying two labels impairs the cellular uptake of membrane translocation sequence peptide conjugates.

By contrast, conjugate C3, consisting of the N-myristoylated conjugate C2, showed uptake into up to 70% of

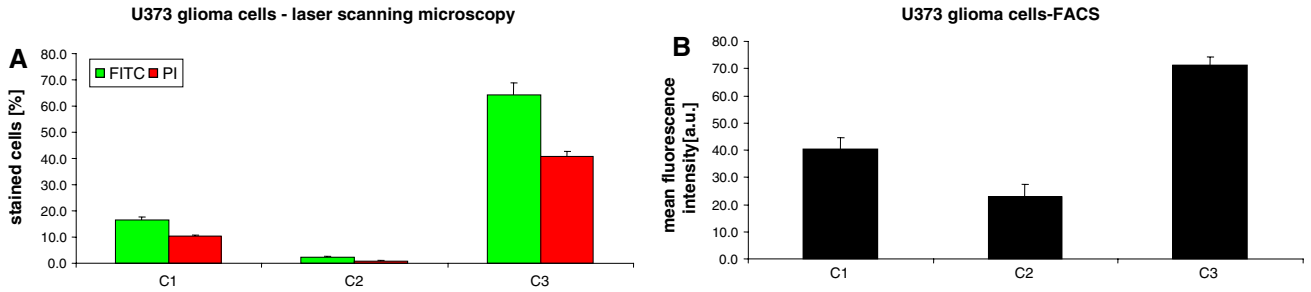

Fig. 2 **a** Percentage of FITC and PI stained cells after incubation with the conjugates C1–C3 (260 μM). Conjugate C1 showed a relatively low number of cells stained with FITC and PI (FITC: 16–18%, PI: 10–11%). FITC and PI staining ratios with conjugate C2 were even lower (FITC: 2–3%, PI: 0–1%). Incubation with conjugate C3 resulted in strong FITC and PI staining (FITC: 60–69%, PI: 39–43%). The examinations were performed three times. The standard deviation of the mean is depicted. **b** FACS (fluorescence activated cell sorting) analysis showed lowest mean fluorescence intensity after incubation with conjugate C2. Mean fluorescence of cells incubated with conjugate C1 was 1.5- to 1.8-fold higher if compared to C2. Conjugate C3 showed the highest mean fluorescence. Its value was roughly 3-fold the value for conjugate C2. The FACS analysis was performed in triplicate. Mean values and standard deviation are displayed

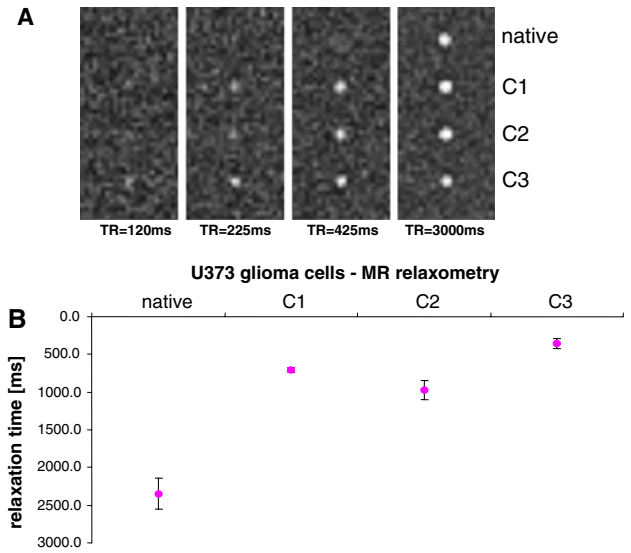

Fig. 3 **a** MR relaxometry of U373 glioma cells (about 6×10^6 cells per sample) incubated with conjugates C1–C3 (260 μM) and PBS as native control. T1-images with different TR-values are exemplarily shown (TR = 120, 225, 425, 3,000 ms). The sample of cells incubated with conjugate C3 was visible first at TR = 120 ms. At TR = 225 ms, the C3 signal is already quite strong. The signal for the C1 sample is clearly visible and a trace signal for the C2 sample can be discerned. At TR = 425 ms, all three conjugate samples C1–C3 are clearly visible while there is still no sign of the native control. Finally at TR = 3,000 ms all samples are visible. **b** T1 relaxation times of U373 glioma cells after incubation with PBS alone and conjugates C1–C3. The *y*-axis is inverted to reflect the fact, that the lowest T1 relaxation times indicate the strongest uptake of contrast agent. The native control shows by far the longest T1 relaxation time (lowest intensity). The sample incubated with C3 presented with the lowest T1 relaxation time of about 360 ms. The sample with conjugate C1 came next with a T1 relaxation time of about 710 ms. C2 was last with a T1 relaxation time of about 975 ms. The examinations were performed three times. The standard deviation from the mean is depicted

cells. Loss of N-myristoylation has been shown to eliminate membrane targeting of membrane associated proteins, e.g. the cGMP-dependent protein kinase II (Vaandrager et al. 1996), and biophysical examinations revealed that the myristoyl-residue can act as a membrane anchor (Sankaram 1994; Desmeules et al. 2002).

Considering this, an increased uptake of C3 as well as association of the conjugate with biological membranes was to be expected. This could be confirmed by our results of confocal laser scanning microscopy, MR relaxometry and FACS.

Surprisingly, even cells within one sample reacted differently towards the conjugates. Even conjugate C3 failed to stain all cells. This indicates that uptake may depend on cell cycle stage as has already been shown for nuclear uptake (Feldherr and Akin, 1990) or on some other kind of cell heterogeneity. The composition of the cell membrane is probably different depending on the cell cycle stage or may even differ amongst the individual cells of a specific cell line.

Another interesting finding was the difference in cell viability after incubation with the three conjugates.

The release of toxic free gadolinium from the complex is a rather unlikely cause for cell death caused by conjugate C3, as the Gd-DOTA complex is known to be very stable with a half-life of 4,000 h (pH2) (Lukes et al. 2001; Magerstadt et al. 1986). The vast difference in cell death rates between the conjugates negates this theory, because the concentration of the Gd-DOTA complex is the same for all three conjugates.

It is known that the HIV-1 Tat peptide may induce apoptosis in hippocampal cells (Kruman et al. 1998). So cell death after incubation with conjugates C2 and C3 could be drawn back to HIV-1 Tat's apoptotic properties. But as conjugate C2 showed very low cytotoxic effect, this explanation can be excluded, too.

It is probable that cell death occurs as an effect of conjugate uptake and happens through membrane disruption. This can be deduced from a constant ratio of nonviable to stained cells (approximately 3 out of 5 cells

stained with all three conjugates were nonviable). Apparently, N-myristoylation does not directly increase conjugate cytotoxicity but only indirectly via higher total conjugate uptake.

While the Antennapedia conjugate C1 stained both the cytoplasm and the cell nucleus, we expected predominant nuclear staining with the HIV-1 Tat peptide conjugates C2 and C3 based on previous reports (Vivès et al. 1997). However, no clear staining pattern was found for conjugate C2, but cells incubated with conjugate C3 clearly showed stained nucleoli and membranes.

Conclusion

N-myristoylation represents a promising strategy for enhancement of cellular uptake of dual labelled peptide conjugates. Due to the fact that the conjugates' cytotoxic properties correlate with the cellular uptake and thus with the MRI signal intensity, such bimodal conjugates could be of great value for future intraoperative tumor imaging combined with chemotherapy.

Acknowledgment The study was supported by the Hertie-Foundation for Brain Research.

References

Bhorade R, Weissleder R, Nakakoshi T, Moore A, Tung CH (2000) Macrocyclic chelators with paramagnetic cations are internalized into mammalian cells via a HIV-tat derived membrane translocation peptide. Bioconjug Chem 11:301–305

Christiaens B, Grooten J, Reusens M, Joliot A, Goethals M, Vandekerckhove J, Prochiantz A, Rosseneu M (2004) Membrane interaction and cellular internalization of penetratin peptides. Eur J Biochem 271:1187–1197

Derossi D, Joliot AH, Chassaing G, Prochiantz A (1994) The third helix of the Antennapedia homeodomain translocates through biological membranes. J Biol Chem 269:10444–10450

Derossi D, Calvet S, Trembleau A, Brunissen A, Chassaing G, Prochiantz A (1996) Cell internalization of the third helix of the Antennapedia homeodomain is receptor-independent. J Biol Chem 271:18188–18193

Desmeules P, Grandbois M, Bondarenko VA, Yamazaki A, Salesse C (2002) Measurement of membrane binding between recoverin, a calcium-myristoyl witch protein, and lipid bilayers by AFM-based force spectroscopy. Biophys J 82:3343–3350

Feldherr CM, Akin D (1990) The permeability of the nuclear envelope in dividing and nondividing cell cultures. J Cell Biol 111:1–8

Kruman II, Nath A, Mattson MP (1998) HIV-1 protein Tat induces apoptosis of hippocampal neurons by a mechanism involving caspase activation, calcium overload, and oxidative stress. Exp Neurol 154:276–288

Le Mignon MM, Chambon C, Warrington S, Davies R, Bonnemain B (1990) Gd-DOTA. Pharmacokinetics and tolerability after intravenous injection into healthy volunteers. Invest Radiol 25:933–937

Lukes I, Kotek J, Vojtisek P, Hermann P (2001) Complexes of tetraazacycles bearing methylphosphinic/phosphonic acid pendant arms with copper(II), zinc(II) and lanthanides(III). A comparison with their acetic acid analogues. Coord Chem Rev 216:287–312

Magerstadt M, Gansow OA, Brechbiel MW, Colcher D, Baltzer L, Knop RH, Girton ME, Naegele M (1986) Gd(DOTA): an alternative to Gd(DTPA) as a T1, 2 relaxation agent for NMR imaging or spectroscopy. Magn Reson Med 3:808–812

Minnicozzi M, Ramirez MM, Egan RW, Gleich GJ, Kobayashi I, Kim D, Duran WN (1995) Polyarginine and eosinophil-derived major basic protein increase microvascular permeability independently of histamine or nitric oxide release. Microvasc Res 50:56–70

Nelson AR, Borland L, Allbritton NL, Sims CE (2007) Myristoyl-based transport of peptides into living cells. Biochemistry 46:14771–14781

Prantner AM, Sharma V, Garbow JR, Piwnica-Worms D (2003) Synthesis and characterization of a Gd-DOTA-D-permeation peptide for magnetic resonance relaxation enhancement of intracellular targets. Mol Imag 2:333–341

Sankaram MB (1994) Membrane interaction of small N-myristoylated peptides: implications for membraneanchoring and protein-protein association. Biophys J 67:105–112

Sturzu A, Regenbogen M, Klose U, Echner H, Gharabaghi A, Heckl S (2008) Novel dual labelled nucleus-directed conjugates containing correct and mutant nuclear localisation sequences. Eur J Pharm Sci 22:207–215

Vaandrager AB, Ehlert EM, Jarchau T, Lohmann SM, de Jonge HR (1996) N-terminal myristoylation is required for membrane localization of cGMP-dependent protein kinase type II. J Biol Chem 271:7025–7029

Vivès E, Brodin P, Lebleu B (1997) A truncated HIV-1 Tat protein basic domain rapidly translocates through theplasma membrane and accumulates in the cell nucleus. J Biol Chem 272:16010–16017

Wender PA, Mitchell DJ, Pattabiraman K, Pelkey ET, Steinman L, Rothbard JB (2000) The design, synthesis, and evaluation of molecules that enable or enhance cellular uptake: peptoid molecular transporters. Proc Natl Acad Sci USA 97:13003–13008